A DNA-Inspired Synthetic Ion Channel Based on G−C Base Pairing

Rabindra Nath Das,[†,‡] Y. Pavan Kumar,[‡] Ole Mathis Schütte,[§] Claudia Steinem,*[,§] and Jyotirmayee Dash*[,†,‡]

[†]Department of Organic Chemistry, Indian Association for the Cultivation of Science, Jadavpur, Kolkata, West Bengal 700032, India

[‡]Department of Chemical Sciences, Indian Institute of Science Education and Research Kolkata, Mohanpur, West Bengal 741246, India

[§]Institute of Organic and Biomolecular Chemistry, Georg-August University Göttingen, Tammannstr. 2, Göttingen, Lower Saxony 37077, Germany

S *Supporting Information*

ABSTRACT: A dinucleoside containing guanosine and cytidine at the end groups has been prepared using a modular one-pot azide−alkyne cycloaddition. Single channel analysis showed that this dinucleoside predominantly forms large channels with 2.9 nS conductance for the transport of potassium ions across a phospholipid bilayer. Transmission electron microscopy, atomic force microscopy, and circular dichroism spectroscopy studies reveal that this dinucleoside can spontaneously associate through Watson−Crick canonical H-bonding and $\pi-\pi$ stacking to form stable supramolecular nanostructures. Most importantly, the ion channel activity of this G−C dinucleoside can be inhibited using the nucleobase cytosine.

Natural ion channels are essential for life processes.[1] They are high-molecular weight pore forming proteins that promote transport of ions across biological membranes. Inspired by nature, there is an increased interest in developing artificial ion channels that can mimic the fundamental functions of natural ion channels.[2−5] The creation of artificial ion channels may improve our understanding of natural ion channels and open up possible applications in materials and biological sciences. Therefore, it is important to devise easily synthesizable, cost-effective, and biocompatible transmembrane channels with tailored physiological properties.

While peptide-based synthetic ion channels have been widely studied,[2,3,5] only a few examples of synthetic ion channels based on nucleobases have been reported.[6−8] Mostly guanine derivatives have been demonstrated to form synthetic ion channels in the membrane.[7,8] In these examples, guanine can self-assemble in the presence of cations to form macrocyclic G-quartets that further stack to form G-quadruplexes.[7,8] Langecker et al. reported that self-assembled DNA nanostructures can form ion channels in the lipid bilayer.[9]

We intended to utilize self-complementary guanosine (G) and cytidine (C) nucleosides to program biomimetic supramolecular structures in the membrane that can facilitate the transport of ions. Guanosine has ionophoric properties, and in the presence of potassium ions, guanosine can assemble to form G-quadruplexes,[10−12] while guanosine and cytidine can be stabilized by Watson−Crick hydrogen bonds.[13] Synthetic

analogues of the natural G−C hydrogen bonding motifs have been used to assemble supramolecular structures.[13] Additionally, cytidine diphosphate diacylglycerol is the most common natural nucleolipid, which plays an important role in the biosynthesis of membrane phospholipids.[14]

In an attempt to prove the principle, herein we delineate a modular access to the synthesis of a G−C dinucleoside via a triazole linkage that can spontaneously assemble into stable supramolecular nanostructures with the potential to form ion channels in the membrane and whose conductance can be selectively inhibited. For the synthesis, we incorporated an acetylene unit in guanosine and an azide unit in cytidine (Scheme 1; Supporting Information, Scheme S1). The

**Scheme 1. Modular Synthesis of a G−C Dinucleoside**
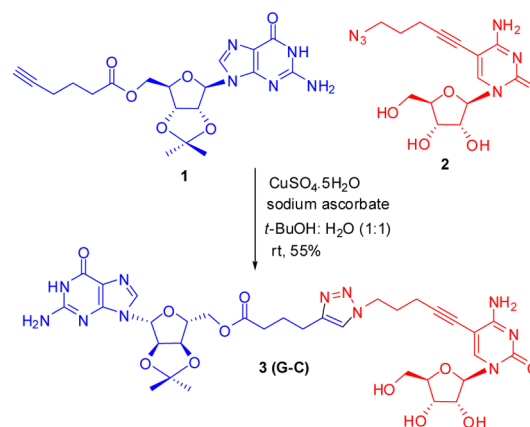
guanosine alkyne **1** underwent smooth Cu(I)-catalyzed azide−alkyne 1,3-dipolar cycloaddition[15] with the azido cytidine **2** using Na-ascorbate and $CuSO_4 \cdot 5H_2O$ in *t*-BuOH/ H_2O (1:1) as solvent to give the triazole-linked guanosine−cytidine dinucleoside **3** (G−C) in 55% yield.

To test its ability to transport the physiologically important cation K^+ across membranes, voltage-clamp experiments were employed on planar solvent-free bilayers in 1 M KCl phosphate (2 mM) buffer at pH 7.4. Planar solvent-free bilayers were produced by spreading giant unilamellar vesicles (GUVs)

consisting of 1,2-diphytanoyl-*sn*-glycero-3-phosphocholine (DPhPC) and cholesterol (9:1) on a small aperture in glass.[16] Current traces were recorded after insertion of G–C dinucleoside into the membrane. Similar to the natural ion channels, synthetic ion channels formed by the G–C dinucleoside exhibit conductance values that appeared and disappeared for several minutes (Figure 1, Figure S1a). The
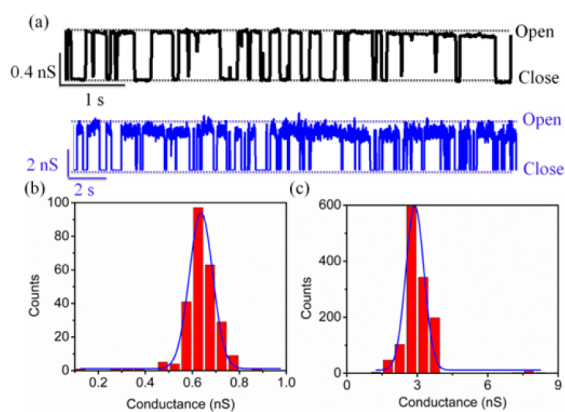
Figure 1. (a) Traces of single-channel recordings obtained by the insertion of G–C dinucleoside (20 μM) to the *cis* side of the chamber after the planar bilayer was formed. Distribution of the two distinct conductance states (1557 events) of G–C dinucleoside: (b) 0.1–1 nS (mean conductance 0.64 ± 0.05 nS) for the conductance trace shown in the top of panel a; (c) 1–8 nS (mean conductance 2.9 ± 0.4 nS) for the conductance trace shown in the bottom of panel a.

histogram of conductance values showed existence of two distinct conductance levels, one around 0.64 nS and one around 2.9 nS. It is noteworthy that large-conductance channels were present in a majority of experiments (80%) with conductance values of 1–8 nS and a mean value of 2.9 nS. G–C also formed channels (20%) with conductance values of 0.1–1 nS with a mean value of 0.64 nS. The presence of distinct channel types indicates the formation of two different species in the membrane. The lifetime of G–C channels spans a wide range from <10 ms to 5 s (Figure S1b). Control experiments showed no measurable conductance in the absence of the G–C dinucleoside. No current changes in the presence of G–C were observed using $BaCl_2$, which suggests an influence of the electrophoretic mobility of the cation or the inability of the G–C channels to adapt to the cation.[17]

Next, we investigated if G–C dinucleoside can induce release of carboxyfluorescein (CF) from vesicles.[18] G–C dinucleoside (4 × 25 μM in DMSO) was added to the CF encapsulating vesicles, and the fluorescence intensity was monitored over time at 520 nm (excitation at 492 nm). A release of the dye from the vesicles would increase its fluorescence intensity and indicate pore formation. Figure 2 shows the fluorescence time course of CF-containing large unilamellar vesicles (LUVs) over a time period of 130 min. No release of CF was observed in the absence of G–C dinucleoside or use of DMSO as a control. In the presence of G–C dinucleoside, a slow increase in fluorescence intensity was observed, which indicates the formation of pores. The value after disruption of the vesicles using Triton-X corresponds to 100% release of CF. G–C dinucleoside-induced CF release was concentration-dependent, and approximately 23% of the entrapped carboxyfluorescein was released at 100 μM concentration of G–C after 2 h.
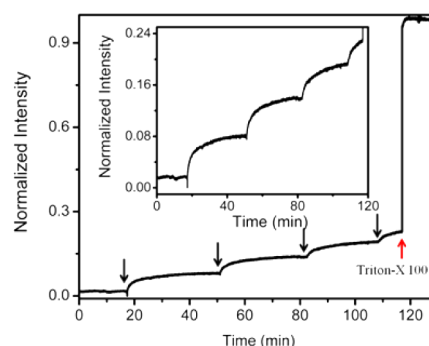
Figure 2. Plot of percentage of CF release from liposomes (DPhPC/cholesterol = 9:1) induced by the G–C dinucleoside (4 × 25 μM) as a function of time. The black arrows indicate the addition of G–C. Complete release of CF was determined after the liposomes were destroyed with Triton X-100 (red arrow).

Transmission electron microscopy (TEM) and atomic force microscopy (AFM) images were taken to investigate possible structure formation due to the self-assembly of G–C dinucleoside. TEM imaging revealed coiled helical filamentous nanostructures in addition to linear nanofibers of width 4.8 nm and ranging up to a few micrometers (Figures 3a and S3). The
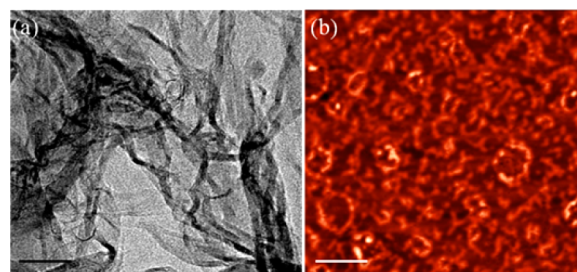
Figure 3. (a) TEM image: scale bar, 50 nm and (b) AFM image: scale bar, 200 nm.

primary nanofibrils were even interconnected to form thick bundles up to 14.9 nm in width. The formation of the higher-order structures is a result of the H-bonded head-to-tail polymeric ability of the dinucleoside as it contains guanosine and cytosine at its two ends (Figure 5). The formation of helical nanofilaments and subsequent bundle formation in TEM may be explained based on iterative intermolecular H-bonding between complementary nucleobases in combination with π–π stacking and hydrophobic interactions (Figure 5), where the triazole ring may contribute to enhanced π–π interactions between two adjacent stacks. Further AFM analysis supported formation of a network of cross-linked fibrils of the G–C with an average height of 5.5 nm (Figures 3b and S4). Powder X-ray diffraction (PXRD) patterns for G–C exhibited a broad peak at $2\theta = 28.9$ ($d = 0.33$ nm), which could be related to guanosine–cytidine stacking between two adjacent vertical G–C stacks (Figure S5). Dynamic light scattering (DLS) also confirmed the aggregation behavior of the dinucleoside in solution with an average diameter of ~28 nm (Figure S6).
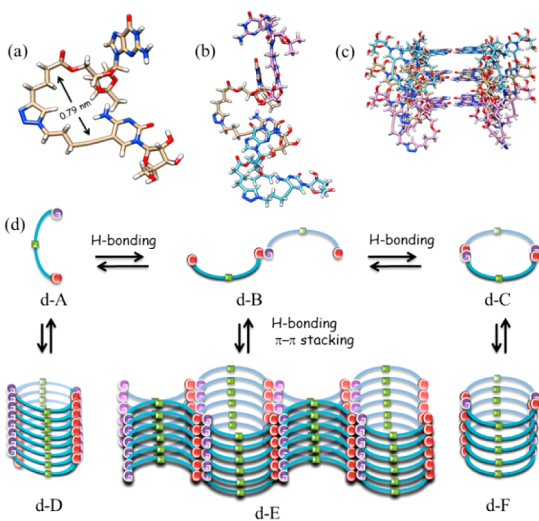
Spectroscopic studies were performed to get insights into the supramolecular assemblies of G–C in the absence or presence of LUV suspensions (Figure 4). The UV spectrum of G–C dinucleoside showed peaks at 247 nm and 278 nm corresponding to the π–π stacking of the nucleobases (Figure 4a). Observation of a shoulder at 306 nm was attributed to the
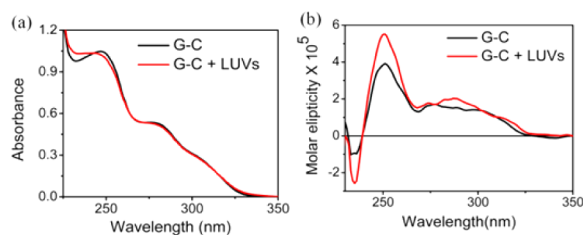
Figure 4. (a) UV and (b) CD spectra of G−C dinucleoside (20 μM) in the absence and in the presence of vesicles in PBS (2.7 mM KCl, 136.9 mM NaCl, 1.5 mM KH_2PO_4, and 8.1 mM Na_2HPO_4, pH 7.4).

$\pi-\pi$ stacking of the triazole ring. The addition of LUV suspensions to a solution of G−C dinucleoside resulted in a marginal hypochromicity of the absorption peak at 247 nm along with a blue shift of about 5 nm, which suggests its interaction with the membrane. Circular dichroism (CD) spectroscopy revealed a negative peak at 235 nm, a positive peak at 250 nm, and a broad positive peak at 288 nm in accordance with the absorption peaks in the corresponding UV spectra, which suggests the presence of supramolecularly oriented chirality of the G−C irrespective of the LUVs (Figure 4b). Moreover, the UV and CD prediction spectra are quite comparable to the experimental UV and CD spectra (Figure S10).

Density functional theory (DFT) structural analysis of the G−C dinucleoside reveals that the triazole containing linker between the two end nucleosides is flexible to make a peripheral pore of 0.79 nm diameter (Figures 5a,d,d-A and
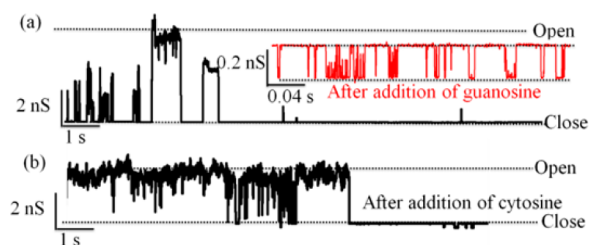
certainly cannot rule out the possibilities where a linear chain of G−C dinucleoside can form helical pores (Figures 5d, d-D and S9). Despite the flexibility of the small linker, the G−C monomer may just self-assemble to form cyclic dimers (Figure 5d, d-C). The cyclic dimers can further self-assemble side-by-side to form aggregated pores (Figures 5d, d-F and S9). The size of these channels is comparable with the known biological nanopores (MspA, α-hemolosyin,VDAC, Table S1).[19]

As the G and C motifs are involved in H-bonding, the triazole ring and the ester carbonyl may weakly coordinate the potassium ion and contribute to the K^+ transport. The slow release of CF can be rationalized as follows: (i) the size of CF (~1 nm) is close to that of these channels; and (ii) the negative charge of CF may lead to repulsion due to the presence of the carbonyl oxygen atom in the G−C dinucleoside. The opening and closing of the channels at an applied potential may be due to the dynamic conformational change in the self-assembly of G−C in the membrane. The observed smaller conductance values (0.1−1 nS) may be explained based on the formation of a "barrel-rosette" model using G-quartets as the basic building blocks (Figure 5c).

Molecular disassembly was investigated primarily by two approaches: (i) competition with guanosine and (ii) inhibition with cytosine. Ion channel blockers/inhibitors are compounds that bind to the pores or break the self-assembly and inhibit the activity of a channel in the membrane. When a solution of guanosine (5 mM) was added to the G−C ion channels in the lipid bilayer, the G−C ion channels conductance of 2.9 nS disappeared, and much smaller conductance values were monitored (Figure 6a), with a mean conductance value of

Figure 5. (a) Energy-minimized structure of G−C monomer obtained using B3LYP/6-31G level (Gaussian03); proposed model the G−C ion channels: (b) oligomer based on G−C base pairing and (c) G-quartet; (d) schematic representation of ion channel formation.

Figure 6. Inhibition of ion channel formed from G−C dinucleoside using (a) guanosine and (b) cytosine.

S8). The end-to-end distance of the lowest energy conformer of the G−C dinucleoside is determined to be 1−1.5 nm (Figure S8). The larger TEM diameter compared to the molecular length of G−C indicates lateral association of the vertically stacked G−C on top of each other. We propose that the presence of a flexible linker between G and C end groups may facilitate "barrel-stave"-type structures with nanopore channels of ~0.79−1.6 nm where the triazole rings and the nucleobases facilitate self-assembly of linear chains to fibrous structures by $\pi-\pi$ stacking (Figure 5b and 5d, d-B, d-E). However, we

0.24 nS and a mean open lifetime of 0.71 s (Figure S2). This smaller conductance can be attributed to the formation of competitive G-quadruplex-type ion channels by guanosine.[7,8] However, a complete disappearance of the G−C ion channel conductance was observed when excess cytosine (5 mM) was added to the lipid bilayers (Figure 6b). CD spectroscopy was used to investigate the structural changes of the G−C channels upon addition of guanosine and cytosine (Figure S7). As the concentration of guanosine was increased, a reduction in the molar ellipticity of all the peaks was observed in a dose-dependent manner until the pores were populated with G-quadruplex scaffolds in the presence of K^+.[8,11] Upon titration with cytosine, several peaks were observed with the disappearance of the negative peak at 235 nm and a positive peak at 250 nm. This suggests that cytosine can induce disassembly of the supramolecular organization of G−C in the membrane.

In summary, we created the first biomimetic artificial transmembrane ion channel construct using a self-complementary G−C dinucleoside. The biomimetic ion channel shows

a dwell-time in the range of seconds and exhibits two distinct conductance levels for potassium ions. A competitive assay with guanosine and channel inhibition with cytosine confirms the role of a G–C hydrogen-bonded framework for channel formation. Contrary to the natural ion channel systems, this synthetic ion channel possesses tunability with flexibilities in choosing functionality and length of the linker.

■ ASSOCIATED CONTENT

Ⓢ Supporting Information

Experimental details, synthetic procedures, ^{1}H NMR and ^{13}C NMR spectra, voltage-clamp experiment traces, AFM, TEM analysis, and CD spectra. This material is available free of charge via the Internet at http://pubs.acs.org.

■ AUTHOR INFORMATION

Corresponding Authors

ocjd@iacs.res.in
csteine@gwdg.de

Notes

The authors declare no competing financial interest.

■ ACKNOWLEDGMENTS

■ REFERENCES

(1) (a) Alberts, B.; Johnson, A.; Lewis, J.; Raff, M.; Roberts, K.; Walter, P. *Molecular Biology of the Cell*, 5th ed.; Garland Science: New York, 2007. (b) Hille, B. *Ion Channels of Excitable Membranes*; Sinauer Associates: Sunderland, MA, 2001.

(2) (a) Szymański, W.; Beierle, J. M.; Kistemaker, H. A. V.; Velema, W. A.; Feringa, B. L. *Chem. Rev.* **2013**, *113*, 6114–6178. (b) Chui, J. K. W.; Fyles, T. M. *Chem. Soc. Rev.* **2012**, *41*, 148–175. (c) Gokel, G. W.; Carasel, I. A. *Chem. Soc. Rev.* **2007**, *36*, 378–389. (d) Sisson, A. L.; Shah, M. R.; Bhosale, S.; Matile, S. *Chem. Soc. Rev.* **2006**, *35*, 1269–1286.

(3) (a) Montenegro, J.; Ghadiri, M. R.; Granja, J. R. *Acc. Chem. Res.* **2013**, *46*, 2955–2965. (b) Reiß, H.; Koer, U. *Acc. Chem. Res.* **2013**, *46*, 2773–2780. (c) Itoh, H.; Inoue, M. *Acc. Chem. Res.* **2013**, *46*, 1567–1578. (d) Otis, F.; Auger, M.; Voyer, N. *Acc. Chem. Res.* **2013**, *46*, 2934–2943. (e) Fyles, T. M. *Acc. Chem. Res.* **2013**, *46*, 2847–2855. (f) Gokel, G. W.; Negin, S. *Acc. Chem. Res.* **2013**, *46*, 2824–2833. (g) Gong, B.; Shao, Z. *Acc. Chem. Res.* **2013**, *46*, 2856–2866.

(4) (a) Otis, F.; Racine-Berthiaume, C.; Voyer, N. *J. Am. Chem. Soc.* **2011**, *133*, 6481–6483. (b) Cazacu, A.; Tong, C.; Van Der Lee, A.; Fyles, T. M.; Barboiu, M. *J. Am. Chem. Soc.* **2006**, *128*, 9541–9548.

(5) For selected examples of peptide-based ionophores: (a) Itoh, H.; Matsuoka, S.; Kreir, M.; Inoue, M. *J. Am. Chem. Soc.* **2012**, *134*, 14011–14018. (b) Sánchez-Quesada, J.; Isler, M. P.; Ghadiri, M. R. *J. Am. Chem. Soc.* **2002**, *124*, 10004–10005. (c) Schlesinger, P. H.; Ferdani, R.; Liu, J.; Pajewska, J.; Pajewski, R.; Saito, M.; Shabany, H.; Gokel, G. W. *J. Am. Chem. Soc.* **2002**, *124*, 1848–1849.

(6) Sakai, N.; Kamikawa, Y.; Nishii, M.; Matsuoka, T.; Kato, T.; Matile, S. *J. Am. Chem. Soc.* **2006**, *128*, 2218–2219.

(7) (a) Ma, L.; Harrell, W. A., Jr.; Davis, J. T. *Org. Lett.* **2009**, *11*, 1599–1602. (b) Ma, L.; Melegari, M.; Colombini, M.; Davis, J. T. *J. Am. Chem. Soc.* **2008**, *130*, 2938–2939.

(8) Kumar, Y. P.; Das, R. N.; Kumar, S.; Schütte, O. M.; Steinem, C.; Dash, J. *Chem.—Eur. J.* **2014**, *20*, 3023–3028.

(9) Langecker, M.; Arnaut, V.; Martin, T. G.; List, J.; Renner, S.; Mayer, M.; Dietz, H.; Simmel, F. C. *Science* **2012**, *338*, 932–936.

(10) (a) Balasubramanian, S.; Hurley, L. H.; Neidle, S. *Nat. Rev. Drug Discovery* **2011**, *10*, 261–275. (b) Collie, G. W.; Parkinson, G. N. *Chem. Soc. Rev.* **2011**, *40*, 5867–5892. (c) Riou, J. F.; Guittat, L.; Mailliet, P.; Laoui, A.; Renou, E.; Petitgenet, O.; Megnin-Chanet, F.; Helene, C.; Mergny, J. L. *Proc. Natl. Acad. Sci. U.S.A.* **2002**, *99*, 263–267.

(11) Davis, J. T. *Angew. Chem., Int. Ed.* **2004**, *43*, 668–698.

(12) (a) Lena, S.; Cremonini, M. A.; Federi-Coni, F.; Gottarelli, G.; Graziano, C.; Laghi, L.; Mariani, P.; Masiero, S.; Pieraccini, S.; Spada, G. P. *Chem.—Eur. J.* **2007**, *13*, 3441–3449. (b) Araki, K.; Yoshikawa, I. *Top. Curr. Chem.* **2005**, *256*, 133–165.

(13) (a) Mascal, M.; Farmer, S. C.; Arnall-Culliford, J. R. *J. Org. Chem.* **2006**, *71*, 8146–8150. (b) Sessler, J. L.; Jayawickramarajah, J.; Sathiosatham, M. *Org. Lett.* **2003**, *5*, 2627–2630. (c) Marsh, A.; Silvestri, M.; Lehn, J. M. *Chem. Comm.* **1996**, 1527–1528.

(14) Allain, V.; Bourgaux, C.; Couvreur, P. *Nucleic Acids Res.* **2012**, *40*, 1891–1903.

(15) Rostovtsev, V. V.; Green, L. G.; Fokin, V. V.; Sharpless, K. B. *Angew. Chem., Int. Ed.* **2002**, *41*, 2596–2599.

(16) (a) Kurz, A.; Bunge, A.; Windeck, A. K.; Rost, M.; Flasche, W.; Arbuzova, A.; Strohbach, D.; Müller, S.; Liebscher, J.; Huster, D.; Herrmann, A. *Angew. Chem., Int. Ed.* **2006**, *45*, 4440–4444. (b) Mathivet, L.; Cribier, S.; Devaux, P. F. *Biophys. J.* **1996**, *70*, 1112–1121.

(17) Johnson, R. P.; Fleming, A. M.; Burrows, C. J.; White, H. S. *J. Phys. Chem. Lett.* **2014**, *5*, 3781–3786.

(18) Ferdani, R.; Li, R.; Pajewski, R.; Pajewska, J.; Winter, R. K.; Gokel, G. W. *Org. Biomol. Chem.* **2007**, *5*, 2423–2432.

(19) (a) Dolder, M.; Zeth, K.; Tittmann, P.; Gross, H.; Welte, W.; Wallimann, T. *J. Struct. Biol.* **1999**, *127*, 64–71. (b) Derrington, I. M.; Butler, T. Z.; Collins, M. D.; Manrao, E.; Pavlenok, M.; Niederweis, M.; Gundlach, J. H. *Proc. Natl. Acad. Sci. U.S.A.* **2010**, *107*, 16060–16065. (c) Venkatesan, B. M.; Bashir, R. *Nat. Nanotechnol.* **2011**, *6*, 615–624.